

Chapter 4

Light Control Films on Portable Displays for Reflective Image Quality Enhancement

The multidirectional asymmetrical microlens array light control film (MAMA-LCF) and random grating light control film (RG-LCF) which can direct light incident from multiple directions collectively for viewing is demonstrated in achieving much enhanced brightness, contrast, viewing angle and uniformity in various portable liquid crystal displays. By using index matching material, the interface reflection is greatly reduced. Through optimized designs, the surface scattering, moiré effect, and color dispersion are also suppressed, thus the image performance is much improved. Moreover, using the well-developed semiconductor and stamp molding fabrication processes, the light control films can be produced economically and accurately in large-volume to effectively enhance image quality for portable LCDs.

4.1 Introduction

Reflective liquid crystal displays (R-LCDs)^[64] are being widely used in portable personal digital assistants and mobile communications. Varieties of new applications, such as super twist nematic LCDs (STN-LCDs)^[65] for mobile phones, polymer dispersed liquid crystal (PDLC)^[66] for smart cards, and cholesteric LCDs (Ch-LCDs)^{[67], [68]} for e-books, have been considered. In these applications, low power consumption, high brightness, high contrast ratio, and low cost are critical. However, most of the reflective LCDs still suffer from inadequate brightness and contrast ratio.

Many methods, for examples, laminating front scattering film^[69] on color STN-LCDs, building rough surface reflector (bump reflector)^[70] on the bottom substrate of PDLC, and using single surface rubbed cell for Ch-LCDs, have been proposed for improving the brightness and the contrast ratio. An unidirectional asymmetrical microlens array light control film (AMA-LCF)^[71] had been proposed to enhance the brightness of reflective LCDs. AMA-LCFs constructed by cutting in the direction of the microlens array diameter to form an off-axis array and then laminating it onto the front surface of reflective LCDs, are effective yet low in cost. As shown in Fig. 4-1, oblique incident light can be reflected to a near-normal viewing zone, yielding significant gain in brightness, and thus, improved image quality, as illustrated in Fig. 4-2.

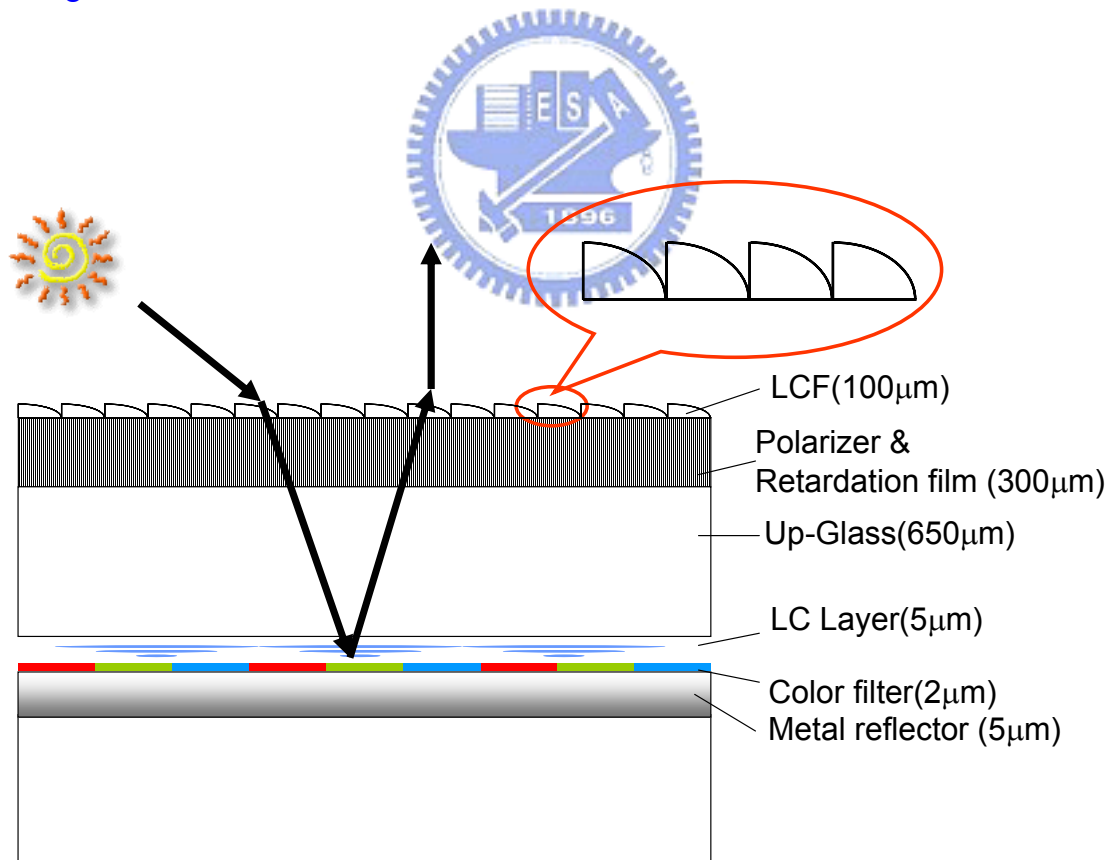


Fig. 4-1. The panel configuration of a reflective display laminating an light control film for collecting and redirecting ambient illuminations.

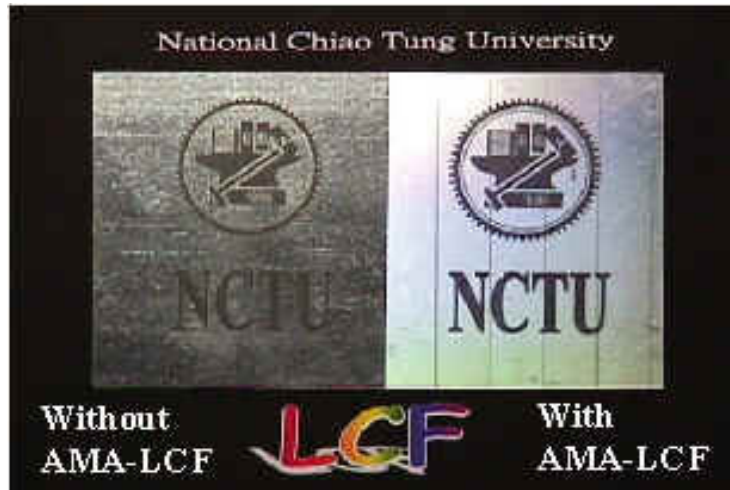


Fig. 4-2. Example photograph of unidirectional AMA-LCF used for brightness enhancement.

However, the AMA-LCF fabricated was for unidirectional ambient illumination. The brightness and contrast ratio enhancement decrease if the light source is not illuminated from the appropriate direction. Therefore, the concept of AMA-LCF was extended to multidirectional asymmetrical microlens array light control film (MAMA-LCF)^{[72], [73]} and random grating light control film (RG-LCF)^[74] so that multiple ambient illuminations can be effectively collected and redirected. MAMA-LCF can focus the reflected light in a specific viewing angle and yield ultra high brightness image with high contrast ratio. By optimizing the grating pitches and orientations of RG-LCF, the reflective light distribution can be well controlled and results in high brightness, wide viewing angle, and high uniformity images. Additionally, simple fabrication and low cost are the other advantages of the light control films. In this chapter, the performances of the light control films on three kinds of reflective LCDs: color STN-LCD, PDLC and Ch-LCD, are demonstrated. Through optimized designs, the image quality of these displays can be significantly improved.

4.2 Optical design of multidirectional AMA-LCF

Multidirectional AMA-LCF (MAMA-LCF) with a fill factor of 100% was designed for a typical ambient environment to significantly improve image quality. In addition to high ambient light utilization, laminating the MAMA-LCF onto various reflective displays can also yield a wide light-collecting angle. Moreover, color dispersion and the moiré effect, which occur with unidirectional AMA-LCFs, are eliminated. Additionally, index matching and surface scattering should also be considered while laminating the light control film onto a reflective LCD.

4.2.1 Color dispersion

In order to avoid color dispersion, the MAMA-LCF structure was modeled as multiple slit gratings of aperture width b and pitch h . Furthermore, color dispersion should be considered in terms of diffraction angle and intensity, which can be calculated from Eqs. (4- 1) and (4- 2)^[75]

$$n\lambda = h \sin \theta \quad \text{for } n = 0, \pm 1, \pm 2, \dots \quad (4- 1)$$

Here, n denotes the order of diffraction and θ is the angle of diffraction. Thus, from Eq. (4- 1), the relationship between wavelength and diffraction angle can be defined. A diffraction intensity I of different order is then derived using

$$I = I_0 \left(\frac{\sin \beta}{\beta} \right)^2 \left(\frac{\sin N\gamma}{N \sin \gamma} \right)^2 \quad (4- 2)$$

where I_0 is the zero-order diffraction intensity, $\beta = 1/2kbsin\theta$ and $\gamma = 1/2khsin\theta$, θ is the diffraction angle which can be derived from Eq. (4- 1), and k is the wave number $2\pi/\lambda$. The factor N renders $I=I_0$ when $\theta=0$. Therefore, by comparing the intensity of different diffraction orders, we can determine which order is relevant, and

then Eq. (4- 1) can be used to derive the dispersion angle. Accordingly, the human pupil and the viewing distance determine the minimum grating period of indistinguishable color dispersion, and are taken into account in the design of MAMA-LCF.

According to the calculated results of Eqs. (4- 1) and (4- 2), the intensity of the second-order diffraction from MAMA-LCF is much lower than that of the first order and can be neglected. We assumed the human pupil to be 3 mm in diameter and the viewing distance to be 30 cm, therefore the difference in the red (R), green (G), and blue (B) diffraction angles should be, at most, 0.573° . The three curves shown in Fig. 4-3 depict the diffraction angle for three different wavelengths and grating periods. It shows that the grating period of less than $25 \mu\text{m}$ may cause a difference in the R, G, and B diffraction angle of larger than 0.5° resulting in visible dispersion. Accordingly, the minimum grating period of MAMA-LCF is $25 \mu\text{m}$.

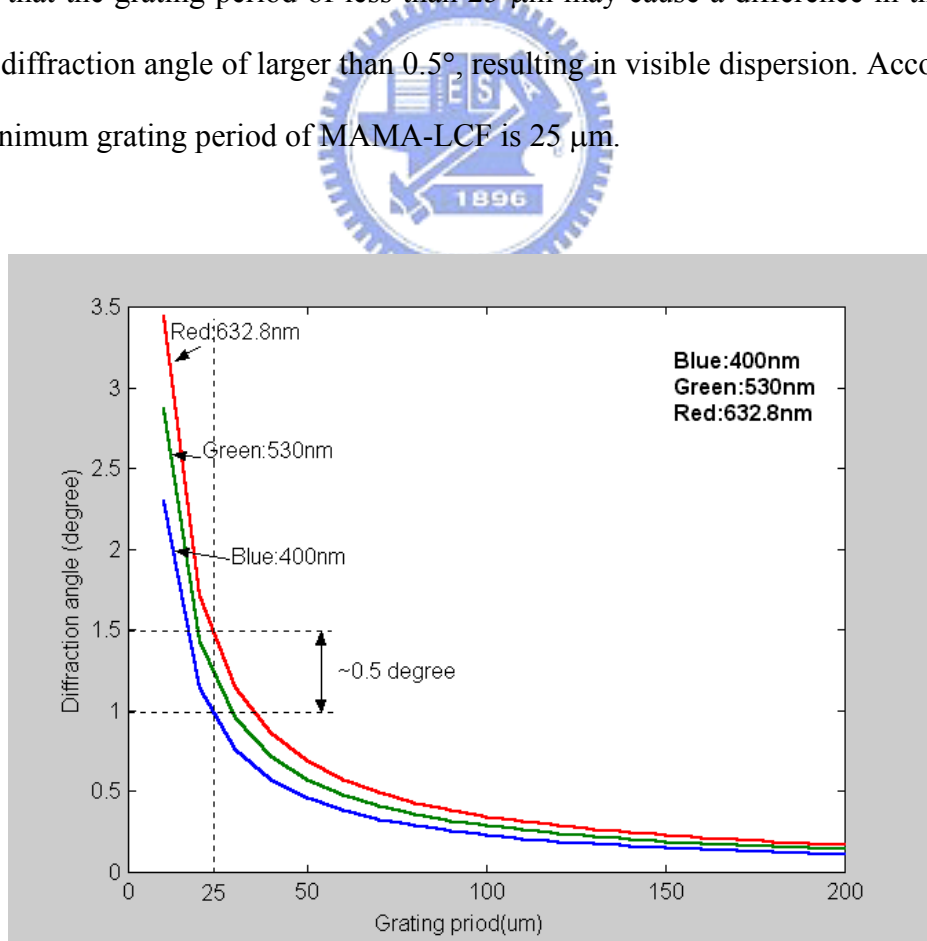


Fig. 4-3. Simulated results of color dispersion.

4.2.2 Moiré pattern

Furthermore, in this design, the moiré pattern^{[76], [77]}, which might occur when periodic LCF structures and periodic pixels of a color filter are superimposed, was also considered. The moiré pattern can be prevented by adopting a specific ratio of the periods of those two structures with a fixed angular difference, which can be calculated by the following equations:

$$q_1 = f_2 / f_1 \quad (4- 3)$$

$$\begin{pmatrix} f_u \\ f_v \end{pmatrix}_{k_1, k_2} = \begin{pmatrix} \cos\alpha & -\sin\alpha \\ \sin\alpha & \cos\alpha \end{pmatrix} \begin{pmatrix} k_1 \\ 0 \end{pmatrix} f_1 + \begin{pmatrix} k_2 \\ 0 \end{pmatrix} q_1 f_1, \quad (4- 4)$$

where f_2 and f_1 are the frequencies of the periodic patterns on the color filter and MAMA-LCF, respectively. The vector (f_u, f_v) denotes the spatial frequency required for the moiré pattern to occur. The angle α is the angular difference between two structures, and (k_1, k_2) are the harmonic terms of each frequency. Thus, the frequency f_{k_1, k_2} and the period T_{k_1, k_2} at which the moiré pattern occurs are given by the sum vector \mathbf{f} :

$$f_{k_1, k_2} = \sqrt{f_{u_{k_1, k_2}}^2 + f_{v_{k_1, k_2}}^2} \quad (4- 5)$$

$$T_{k_1, k_2} = \frac{1}{f_{k_1, k_2}}. \quad (4- 6)$$

The human eyes cannot resolve the moiré pattern with a period of less than 1. Because the frequency of the color filter (f_2) is fixed, the non-moiré frequency (f_1) and the orientation (α) of MAMA-LCF can be derived from eqs. (4- 3) - (4- 6). Then, MAMA-LCF can be designed to have microlenses with multiple orientations, where each microlens has a different pitch and orientation.

The contour map^[77] of the period number for the occurrence of moiré patterns,

based on the calculated results of eqs. (4- 3) - (4- 6), is shown in Fig. 4-4. The X-axis shows the angle between the two periodic structures, the Y-axis shows the ratio of the periods of the two structures, and the numbers on the contour line are the number of periods of the moiré pattern. In this design, the microlenses of MAMA-LCF are oriented in three different orientations and have three different period ratios, (0^0 , 3.0) and ($\pm 45^0$, 2.1), which can prevent the moiré patterns from occurring, as shown in Fig. 4-4.

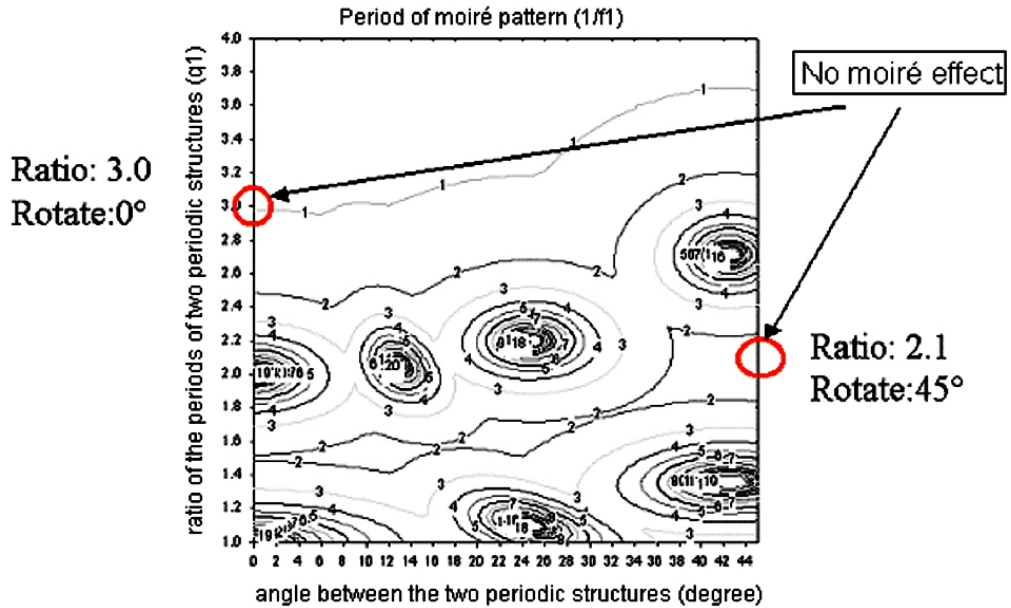


Fig. 4-4. Contour map of occurrence of moiré patterns.

Therefore, the MAMA-LCF shown schematically in Fig. 4-5(b), whose microlenses are rotated in three different orientations (0^0 , $\pm 45^0$) and rearranged into a particular structure, was designed and fabricated. The superimposition of a unidirectional LCF and a color STN-LCD caused several undesirable oblique strips, i.e., moiré patterns, which have been successfully eliminated by using the new MAMA-LCF, as shown in Figs. 4-6(a) and (b). Additionally, to be applicable to a reflective color STN-LCD with pixel size with $210 \mu\text{m} \times 210 \mu\text{m}$, there are more than 50 microlenses within each pixel. Thus, moiré patterns are not visible because the designed structure and the pitch of the microlenses are much smaller than the pixel

size.

From the above calculations, an optimal size and arrangement of microlenses can be determined, so that the MAMA-LCF laminated onto a color STN-LCD can yield high brightness and wide viewing angle without visible color dispersion or the moiré pattern.

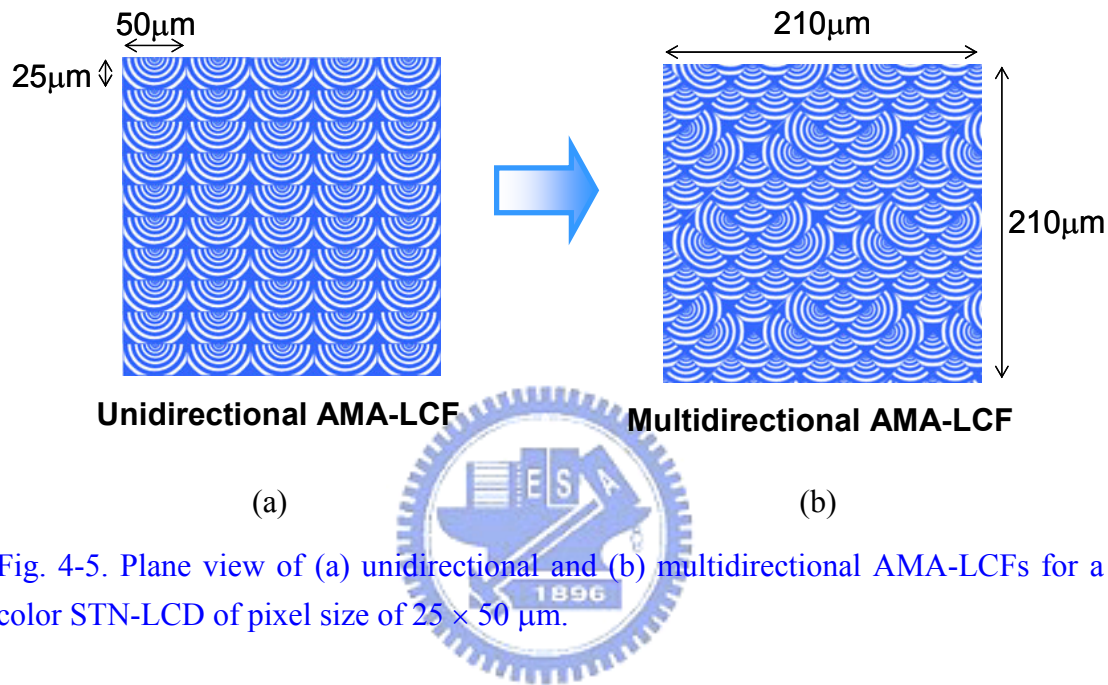


Fig. 4-5. Plane view of (a) unidirectional and (b) multidirectional AMA-LCFs for a color STN-LCD of pixel size of $25 \times 50 \mu\text{m}$.

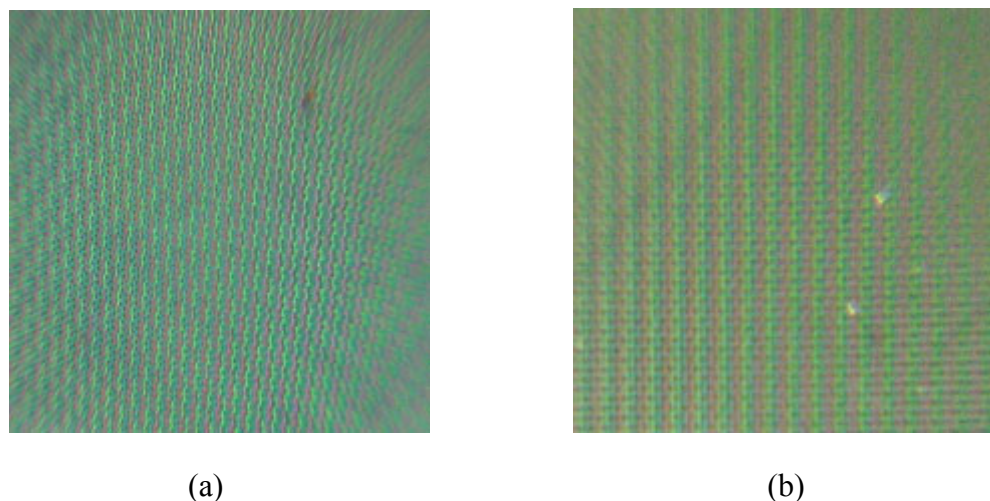


Fig. 4-6. Enlarged photographs of a color STN-LCD with (a) a unidirectional LCF and visible oblique strip moiré patterns, and (b) a multidirectional LCF and non-visible moiré patterns.

4.2.3 Surface scattering

From Fresnel's equation and Snell's law, the surface reflective ratio^[78] between two layers with different refractive index for S wave (TE) and P wave (TM) can be respectively shown as Eqs. (4- 7) and (4- 8):

$$R_s = |r_s|^2 = \left| \left(\cos \theta - \sqrt{n^2 - \sin^2 \theta} \right) / \left(\cos \theta + \sqrt{n^2 - \sin^2 \theta} \right) \right|^2 \quad (4- 7)$$

$$R_p = |r_p|^2 = - \left| \left(n^2 \cos \theta + \sqrt{n^2 - \sin^2 \theta} \right) / \left(n^2 \cos \theta + \sqrt{n^2 - \sin^2 \theta} \right) \right|^2 \quad (4- 8)$$

Here $n = \frac{n_t}{n_i}$ is the relative refractive index of refraction of the refractive index of the incident(n_i) and the transmitted(n_t) media, and θ is the light incident angle. Therefore, the total surface reflective ratio R_{total} is:

$$R_{total} = \sqrt{(I_{is} \cdot R_s)^2 + (I_{ip} \cdot R_p)^2} / \sqrt{(I_{is})^2 + (I_{ip})^2} \quad (4- 9)$$

Where I_{is} and I_{ip} are the intensities of the incident S and P wave, respectively. Assuming the incident light is unpolarized, then $I_{is}=I_{ip}$. Consequently, R_{total} can be simplified to be :

$$R_{total} = \sqrt{(R_s)^2 + (R_p)^2} / \sqrt{2} \quad (4- 10)$$

For example, while the light illuminated on a plastic film of refractive index $n=1.55$ from 30° , the total surface reflection is 5.15%. Compared to the 12.5% reflective light

efficiency of a reflective LCD, as signified in Fig. 4-7, the surface reflection results in very serious degradation to the CR. Additionally, the microlens on MAMA-LCF was approximated by using a four-step Fresnel lens instead of traditional curvature lens. Therefore, the edge of each step may scatter the incident light, which results in increased dark state light leakage and degraded CR.

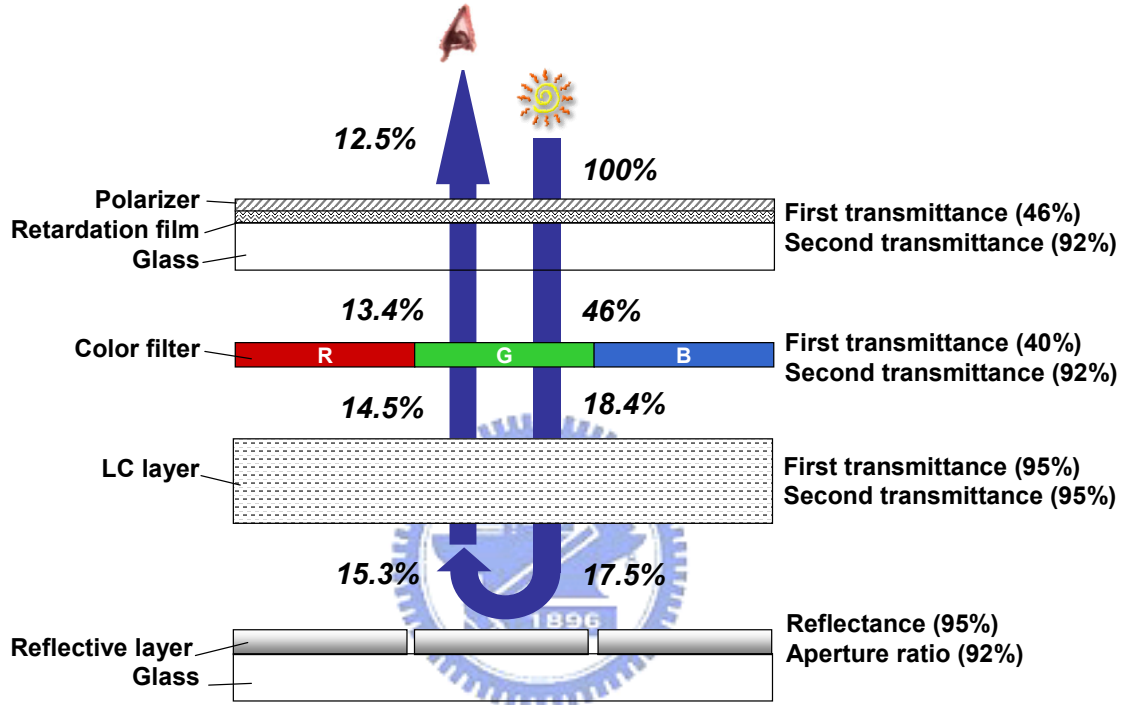


Fig. 4-7. The estimated reflective light efficiency of a reflective LCD.

4.3 Reflective LCDs with MAMA-LCF

Several methods were proposed respectively for laminating the LCF on the following three different kinds of LCDs: reflective color STN, PDLC, and cholesteric, to overcome the above mentioned issues.

4.3.1 Reflective color STN

The designed patterns and system configuration of the MAMA-LCF on reflective

color STN-LCDs are shown schematically in [Fig. 4-8](#), respectively. The pixel size of a reflective color STN-LCD is $210 \mu\text{m} \times 210 \mu\text{m}$ which covers more than 50 microlenses, as shown in [Fig. 4-5](#), thus can avoid moiré patterns. Moreover, coating an index matching material on LCF and laminating it below the polarizer, as depicted in [Fig. 4-8](#), is found to greatly reduce the intensity of interface reflection and front scattering light. As a result, MAMA-LCF laminated below the polarizer should be made of a very low birefringence material to avoid the color shift caused by the retardation effect.

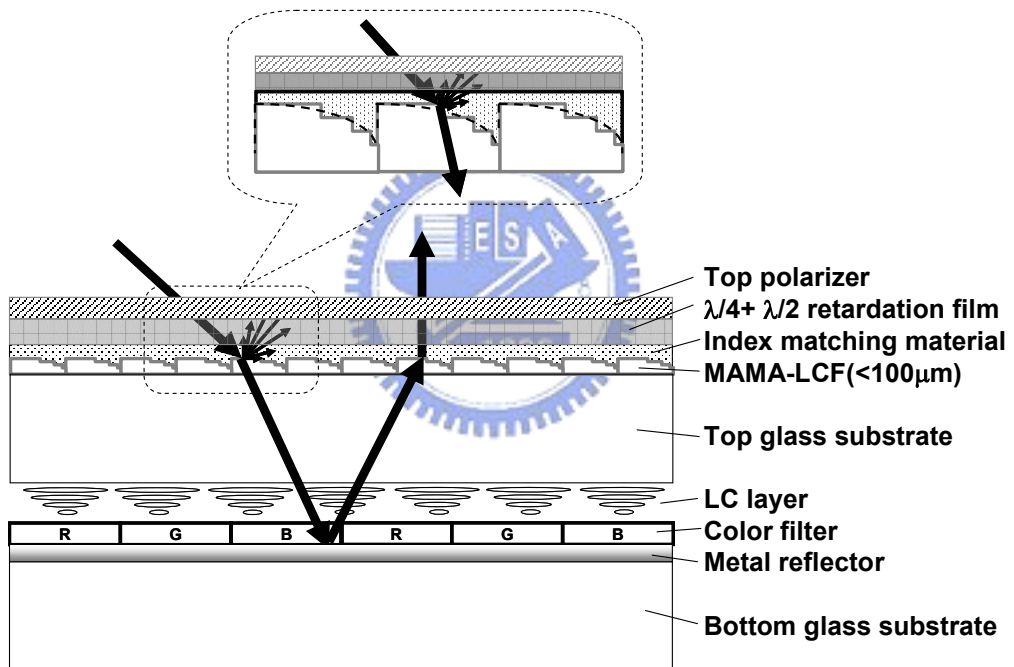


[Fig. 4-8. Schematic plot of system configuration of the MAMA-LCF on a reflective color STN-LCD.](#)

4.3.2 Reflective PDLC

MAMA-LCF is also applicable to the reflective PDLC developed for plastic smart cards. Usually, the MAMA-LCF is laminated on the top surface of PDLC. Under such circumstance, the film modulates the reflected light from the interface of each layer, and deteriorates the blackness of the dark state. Thus, the MAMA-LCF is

preferred to be laminated between the bottom substrate of the plastic PDLC panel and the aluminum reflector with an index matching material coated, as depicted in [Fig. 4-9](#). Moreover, the plastic LCF is flexible and can be easily combined with the plastic PDLC displays.

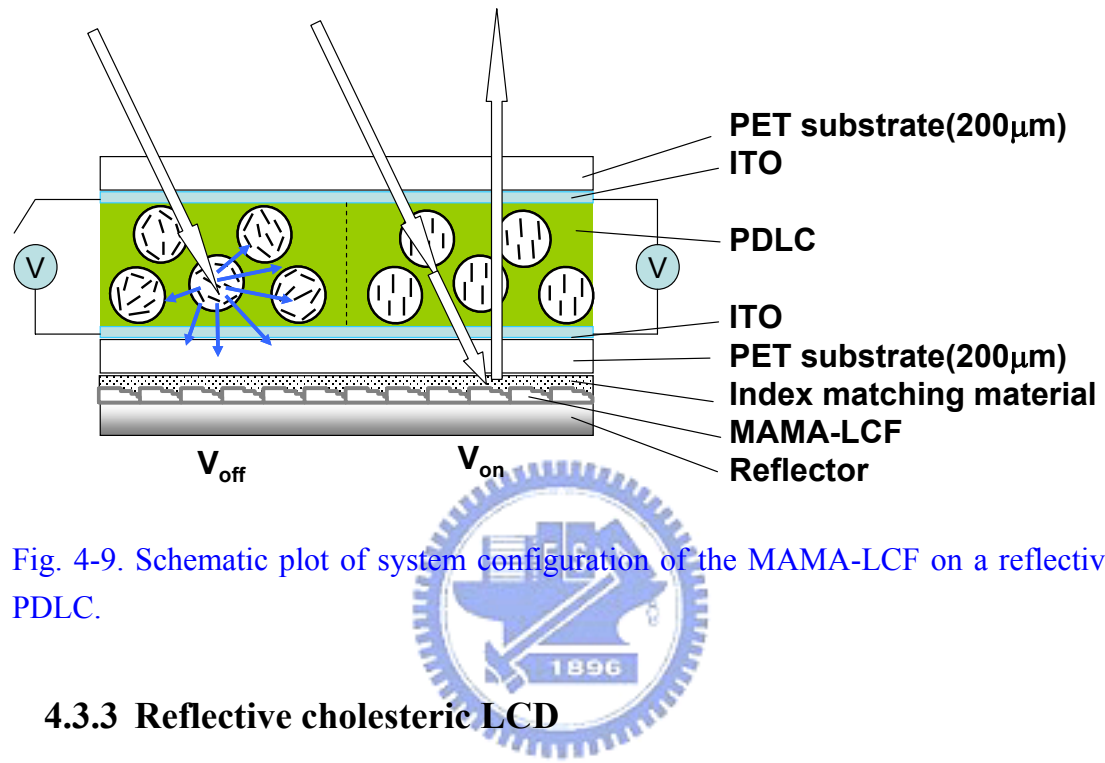


[Fig. 4-9. Schematic plot of system configuration of the MAMA-LCF on a reflective PDLC.](#)

4.3.3 Reflective cholesteric LCD

Cholesteric liquid crystal display (Ch-LCD) is a candidate for electronic-books because of its low power consumption. For a conventional Ch-LCD to achieve wide viewing angle, only the bottom substrate is rubbed and the top plate has no rubbing. The LC directors tilt to different angles. These slightly disordered cholesteric layers help to diffuse the reflected light to a wider viewing zone. The tradeoff of this approach is that the maximum reflectivity is reduced to 35%. On the other hand, the two-surface rubbed cell exhibits a higher (~50%) reflectivity except that its viewing angle is much narrower. Integrating a MAMA-LCF on the two-surface rubbed cell to control viewing angle while preserving high reflectivity shall be more appealing for applications. As shown in [Fig. 4-10](#), the MAMA-LCF helps to direct light to a normal

viewing angle. Moreover, by coating an index matching material can reduce the interface reflections. Benefited from the light control film, the two-surface rubbed Ch-LCD is expected to exhibit high reflectivity in normal viewing direction.

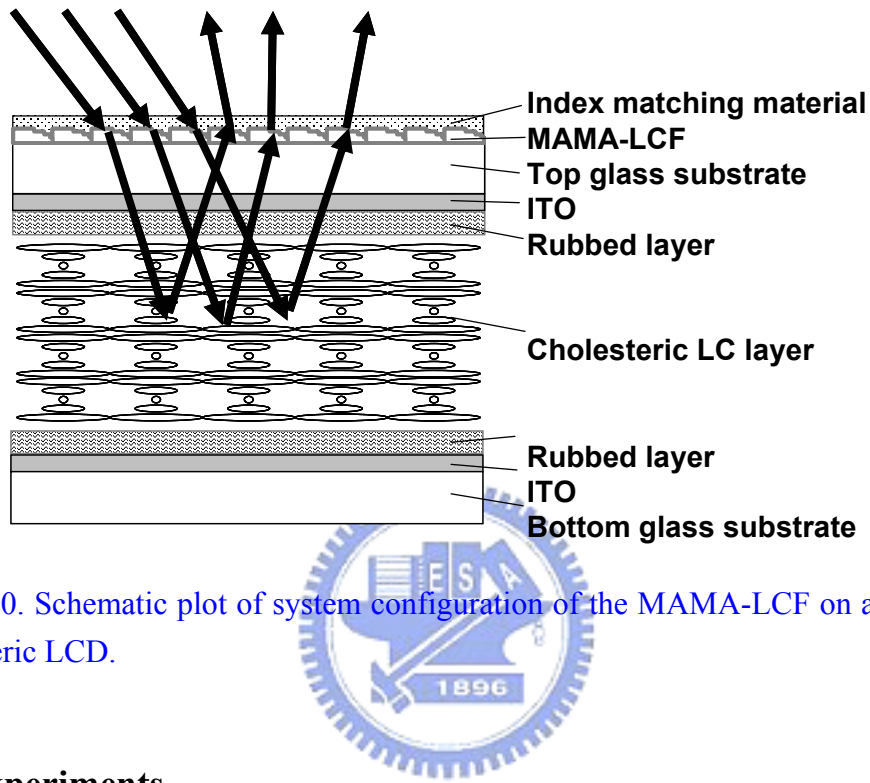


Fig. 4-10. Schematic plot of system configuration of the MAMA-LCF on a reflective cholesteric LCD.

4.4 Experiments

4.4.1 Fabrication of multidirectional AMA-LCF

The asymmetrical microlens array is implemented with a binary Fresnel microlens structure because of its 100% fill factors and the simple fabrication of the asymmetrical microlens pattern. Furthermore, the binary Fresnel microlens is easily fabricated using standard semiconductor processes of photolithography and reactive ion etching (RIE) on a Si wafer utilized as a substrate for making a father mold. Then, the Si substrate is electroplated with a nickel layer to serve as a mother molds. Next, this Si-based structure is duplicated from the mother mold to a transparent plastic film, such as PVC and arton cyclic olefin copolymers (arton-COC), by stamping molding.

The arton-COC film is used for color-STN to avoid the color shift because of its low birefringence. An index matching material, EGC1700 ($n=1.38$) is then spin-coated on the surface of the plastic film to protect the microlens structure and reduce the surface scattering. From Eq. (4), the surface reflection of the MAMA-LCF ($n=1.55$) coated with EGC1700 ($n=1.38$) can be diminished to only 0.41%. Finally, the multidirectional LCF is laminated onto the reflective LCD to realize the control of the distribution of the reflected light. Using these well-developed fabrication processes, a precise microoptical structure can be produced economically and reproducibly in large volume.

4.4.2 LCD parameters

The configurations and the parameters of the different LCDs laminated with multidirectional AMA-LCF are listed in Table. 4-1 and Table. 4-2., respectively. Different focal lengths and the lens configuration of the microlens array can be designed with the optical software ASAP^[79]. The light control effect of MAMA-LCF can be optimized for each LCD depending on their specific needs.

Table. 4-1. Configuration of the test panels.

Code name	Type of the test panel	Index matching material coating	Laminated position of LCF
Bare STN	Color-STN	No	Without LCF
STN - A	Color-STN	No	Above top polarizer
STN - B	Color-STN	Yes	Between top polarizer and top glass substrate
Bare PDLC	PDLC	No	Without LCF
PDLC - A	PDLC	Yes	Between bottom substrate and bottom reflector
Bare Ch-LCD	Ch-LCD	No	Without LCF
Ch-LCD - A	Ch-LCD	Yes	Above top glass substrate

Table. 4-2. Parameters of reflective color-STN, PDLC, and Ch-LCD used.

LC mode	Color STN	PDLC	Cholesteric
LCF	100 μm	100 μm	100 μm
Index matching material	EGC1700 (3 μm)	EGC1700 (3 μm)	EGC1700 (3 μm)
Polarizer	200 μm	None	None
Retardation film	100 μm	None	None
Substrate	Glass (0.6mm)	Plastic-PET(0.1 μm)*	Glass (0.7mm)
ITO (μm)	0.1	0.1	0.1
LC cell gap (μm)	5	6	5
Color filter (μm)	2	None	None
Rubbed layer	Both sides (0.15 μm)	None	Both sides (0.15 μm)
Reflector	Metal reflector	Metal reflector	Cholesteric reflector

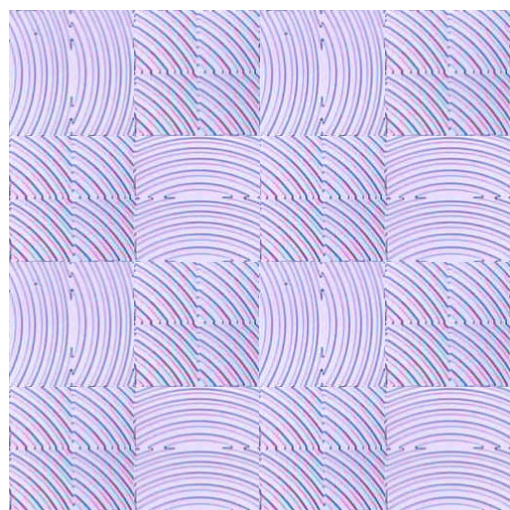
*Polyethylene terephthalate

4.4.3 Evaluation of morphological and optical properties

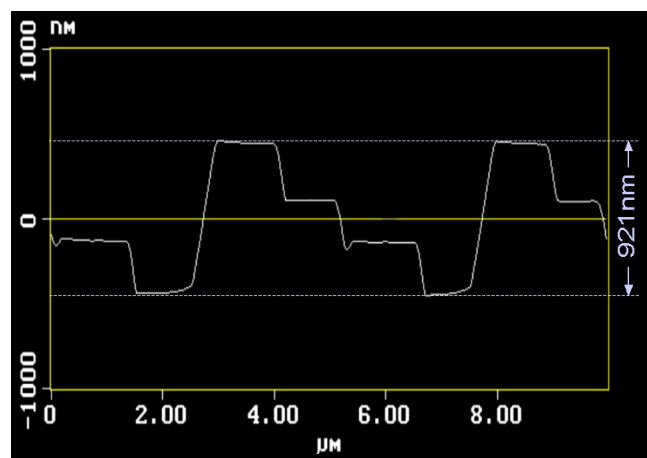
The surface structure and cross-sectional profile of MAMA-LCF were examined using a HITACHI S-4000 SEM and a Di Dimension 3100 AFM, respectively. To measure the reflective brightness and contrast ratio, a single incident light was fixed at -30° as an ambient light, and the reflected light was detected by using ELDIM EZContrast 160R at the effective viewing angle from 0° to 40° . Evaluating the effect of surface reflection, a conoscopic system, ELDIM EZContrast 160R, which can measure $\pm 80^\circ$ viewing cone were also used with a -30° illumination.

4.5 Experimental results of MAMA-LCF

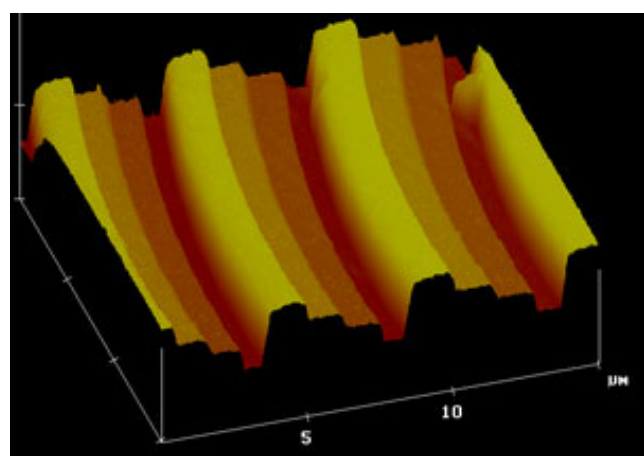
A four-level Fresnel microlens with three different orientations was fabricated. Fig. 4-11 show the plane view, cross-sectional profile and 3D view of the microlens array structure. The depth of the microlens array structure was 921nm, as shown in Fig. 4-11(b), and the fabrication tolerance was better than 1.8% for the designed depth of 930 nm.



(a)



(b)



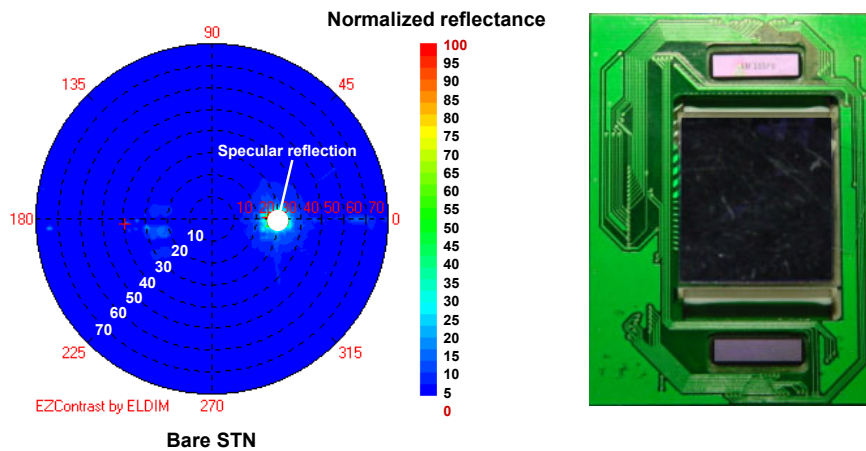
(c)

Fig. 4-11. (a) Plane view, (b) cross-sectional profile, and (c) 3D view of the asymmetrical microlens array structure.

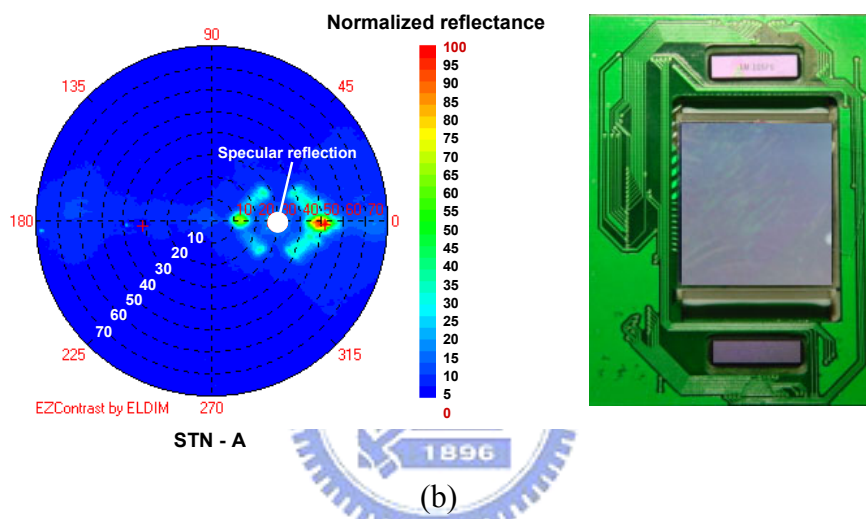
4.5.1 Surface reflection of MAMA-LCF

In order to observe the surface reflection induced by MAMA-LCF, test panels of reflective color-STN with MAMA-LCF laminated were measured. The test panels were in a dark state with a collimated light illuminated from -30° , thus, the specular reflection occurred at 30° , as the white spot shown in [Fig. 4-12](#). The reflectivity of the panels were measured and plotted in polar coordinate to reveal the effect of surface reflection. The measured results of bare STN, STN-A, and STN-B are shown in the left part of [Figs. 4-12\(a\), \(b\) and \(c\)](#), respectively, and the right part displayed the photos of the dark state image of the three test panels taken from the normal viewing angles.

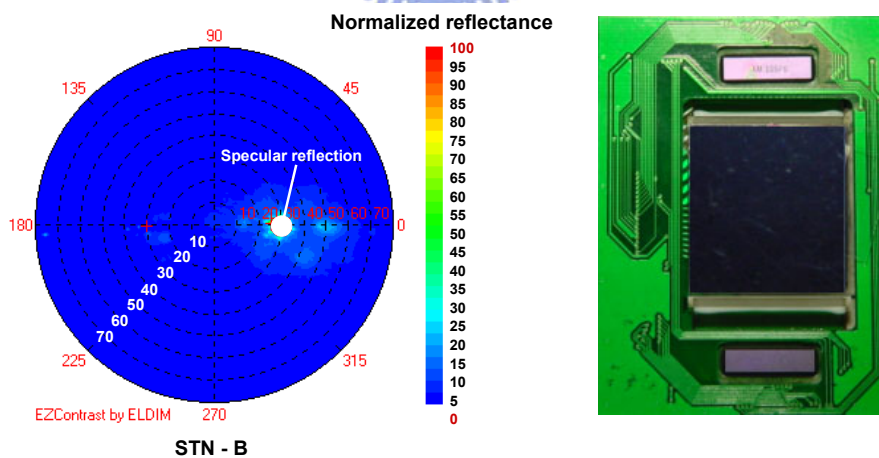
Obviously, both the measured result and the photo of bare STN reveal that the panel can display a very dark image in the viewing region. However, from [Fig. 4-12 \(b\)](#), the reflective light of the dark state of STN-A has noticeably crescent distribution because the LCF was not coated with an index matching material thus the interface reflection efficiency was higher to 5.15%. The interface reflective light was modified by the Fresnel lenses of the LCF, and be directed into the viewing region as the crescent distribution to increase the brightness in the dark state of STN-A, as the photo shown in [Fig. 4-12\(b\)](#). Additionally, the edge of each step of the four-step Fresnel lenses causes surface scattering, as the dark gray area shown in the polar plot of [Fig. 4-12\(b\)](#), which also degrades the image quality at large viewing angle. By using the configuration of STN-B, where MAMA-LCF was coated an index matching material (EGC1700, $n=1.38$) to reduce the interface reflection and laminated below the polarizer to decrease the surface scattering, the darkness of the panel was greatly improved, as shown in the photo of [Fig. 4-12\(c\)](#).



(a)



(b)



(c)

Fig. 4-12. Measured reflectivity (left part) and photos (right part) of the dark state image of (a) Bare STN, (b) STN-A, and (c) STN-B.

MAMA-LCF coated with index matching material was also used for PDLC and Ch-LCD, where the measured dark state reflectance polar plots of the two LCDs are shown in [Figs. 4-13\(a\) and \(b\)](#), respectively. These two devices are non-polarized displays, thus the LCF for PDLC was laminated between the bottom substrate and reflector to decrease the surface scattering. The reflector of Ch-LCD, however, is the LC cell itself. Therefore, LCF can only be added on the top surface of the Ch-LCD that the interface reflection can be reduced by coating an index matching material, yet the surface scattering is slightly visible while displaying the dark state image.

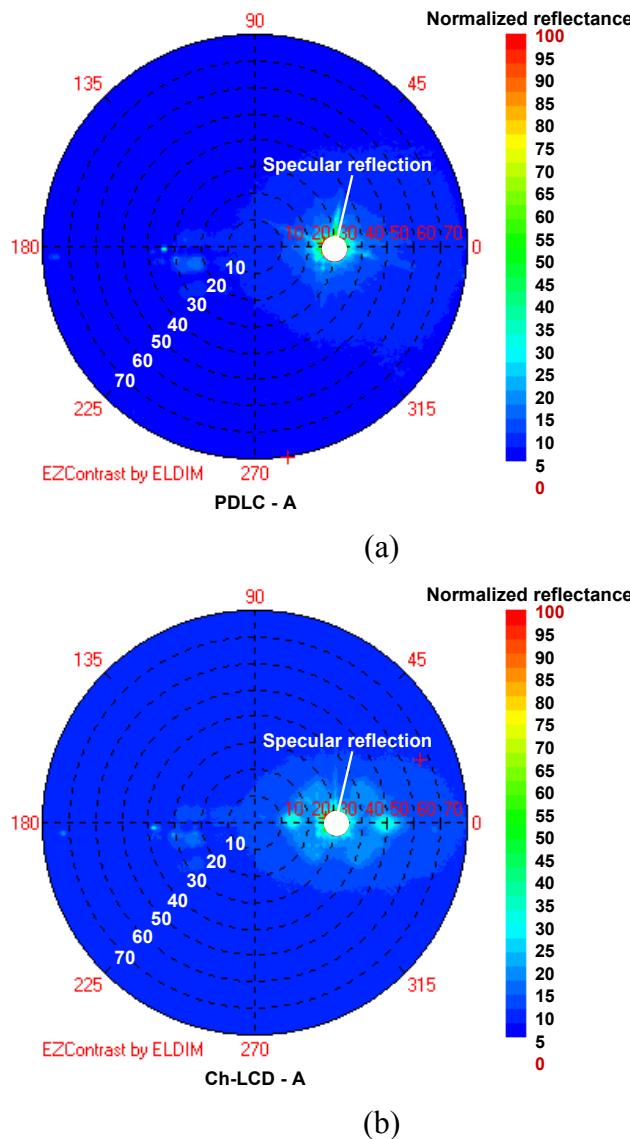


[Fig. 4-13. Measured results of the dark state reflectance of \(a\) PDLC-A and \(b\) Ch-LCD-A.](#)

4.5.2 Image improvement by MAMA-LCF

By coating an index matching material on the MAMA-LCF, the intensity of surface reflection can be much reduced to improve the display quality of dark state image. Thus, the new configuration of the three display panels, STN-B, PDLC-A, and Ch-LCD-A, were measured and compared with the bare test panels. The measured angular-dependent reflectivity and CR of the reflective color-STN, PDLC and cholesteric panels are shown in [Figs. 4-14 to 4-16](#), respectively. For a collimated illumination from -30° , the specular reflection occurs at 30° . At this angle, although the reflectivity is high, CR is poor. Adding a MAMA-LCF not only shifts the peak reflectance of the color-STN panel from 30° to 15° , but also enhances reflectivity by $\sim 1.5X$ over the MgO standard white (Solid line, [Fig. 4-14\(a\)](#)). Since the LCF was coated with an index matching material, EGC1700 ($n=1.38$) and laminated below the top polarizer, the surface reflection is reduced and the CR is increased, as the solid line shown in [Fig. 4-14\(b\)](#), where CR is higher than 10 within viewing angles of 0° to 18° with a peak value of 15. Therefore, MAMA-LCF covered by EGC1700 and adhesive below the top polarizer can provide an image with good CR and high brightness in the viewing region.

Similarly, the reflectance profile of a PDLC sample also reveals that laminating the LCF on the bottom side of the reflective PDLC (PDLC – A) yields a very high brightness (2.8X of MgO) with maximum CR $\sim 23:1$ in the viewing angle 14° , as shown in [Figs. 4-15\(a\) and \(b\)](#). In the Ch-LCD experiments, two cells using E48 LC doped with ZLI-811 chiral agent, which has peak wavelength at green, were used. The back side of the cell was painted black for improving CR. The MAMA-LCF was coated with EGC1700 and laminated on the top surface of the Ch-LCD cell. [Fig. 4-16](#) plots the measured reflectance and contrast ratio of the two-surface buffed Ch-LCD

with and without MAMA-LCF. The Ch-LCD with LCF (solid line) shows a higher reflectance in the 0^0 - 20^0 viewing zone. At 14^0 , the light control film enhances the display brightness by a factor of 2.8 to that of MgO standard white. Additionally, CR of the Ch-LCD with MAMA-LCF, depicted as the solid line in Fig. 4-16(b), is increased to 13 at 14^0 .

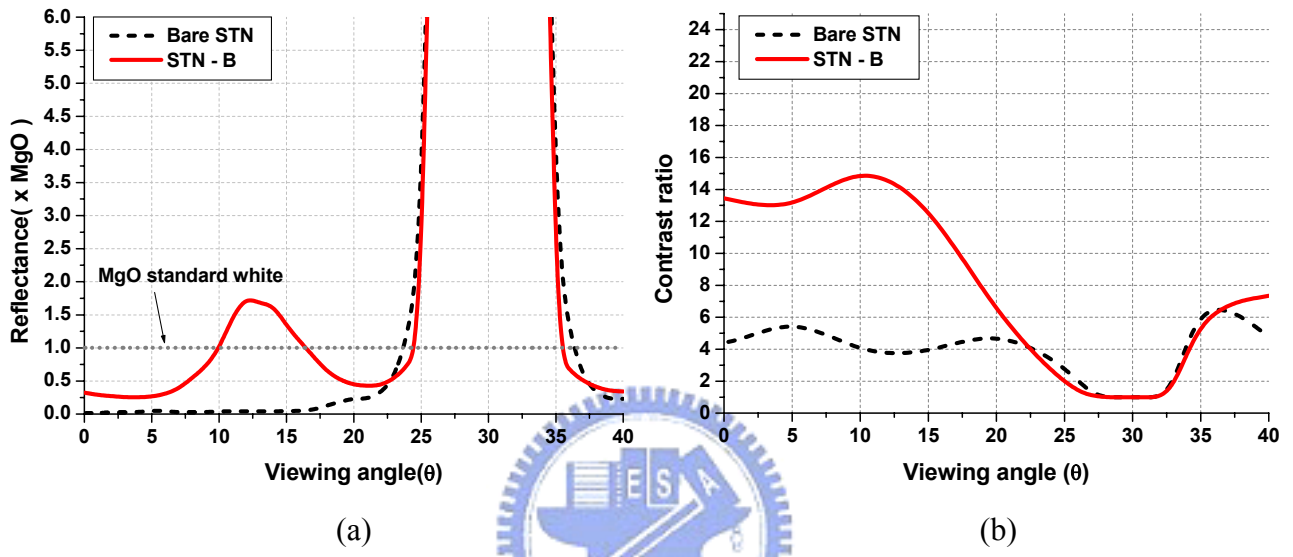


Fig. 4-14. Measured (a) reflectivity and (b) contrast ratio of reflective color-STN LCD as a function of viewing angle under illumination from -30^0 .

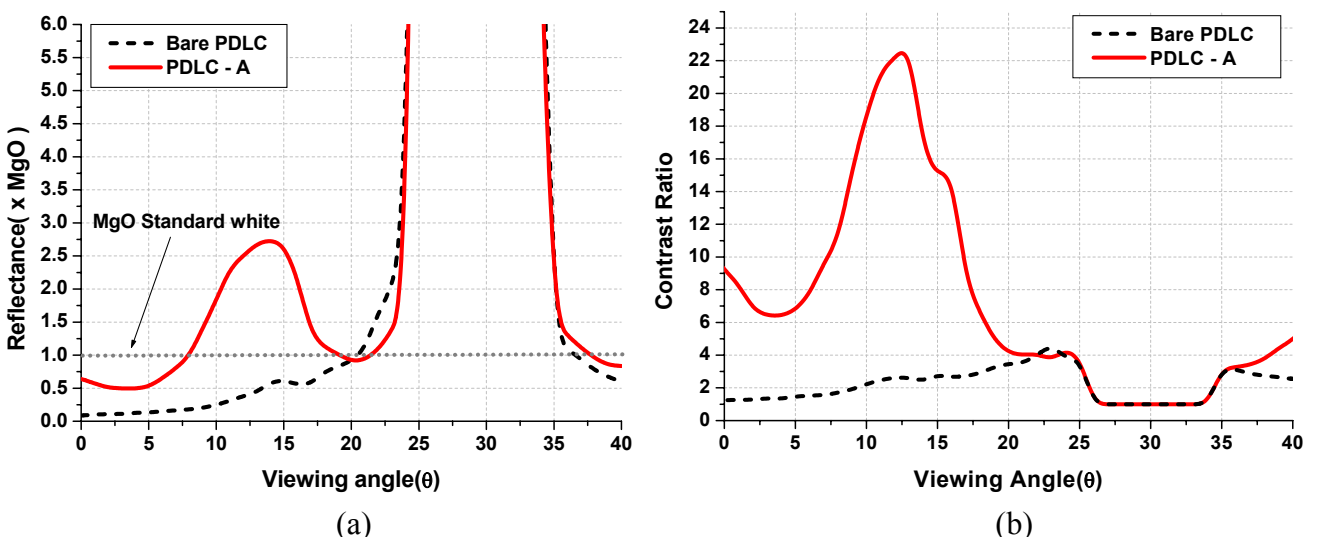


Fig. 4-15. Measured (a) reflectivity and (b) contrast ratio of reflective PDLC as a function of viewing angle under illumination from -30^0 .

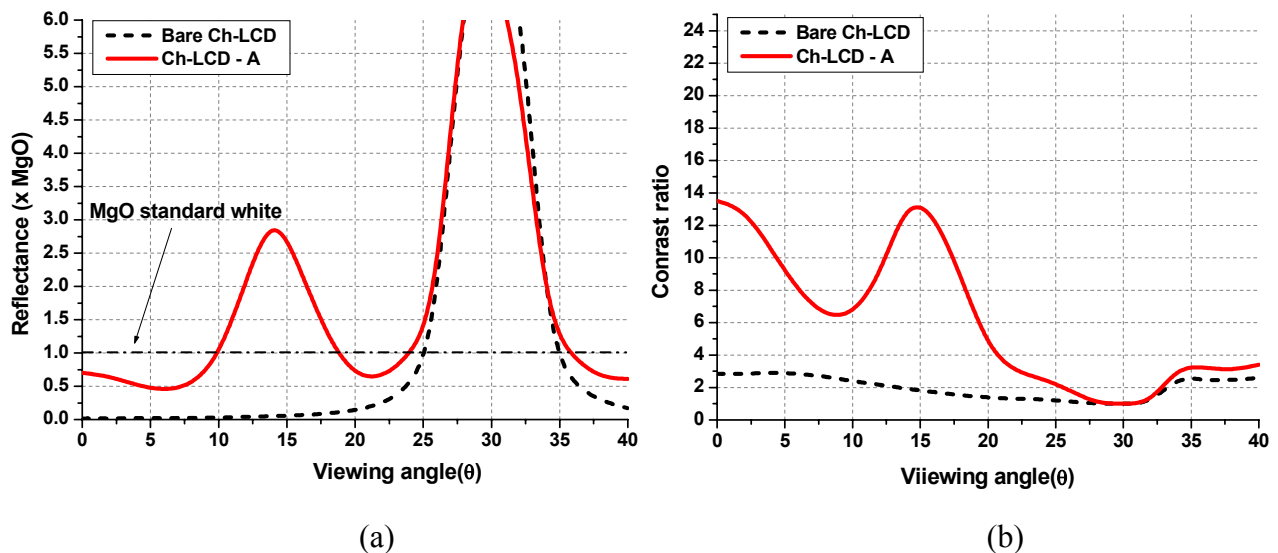
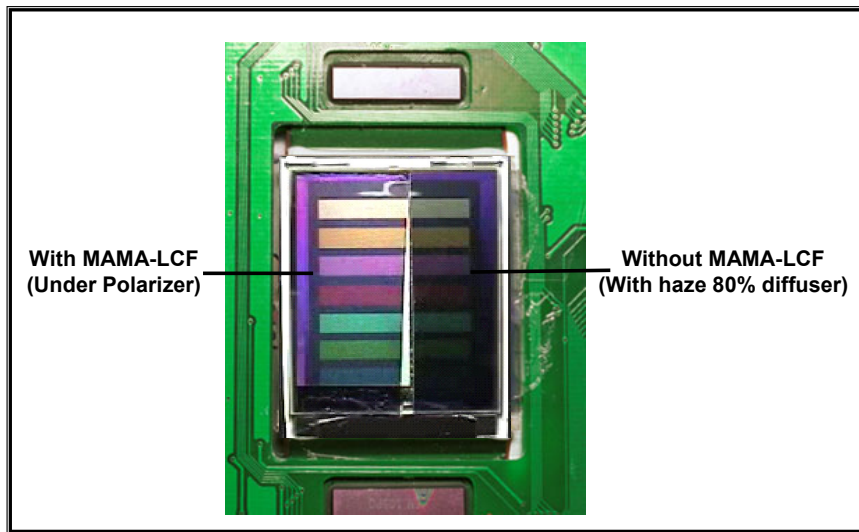


Fig. 4-16. Measured (a) reflectivity and (b) contrast ratio of reflective Ch-LCD as a function of viewing angle under illumination from -30^0 .

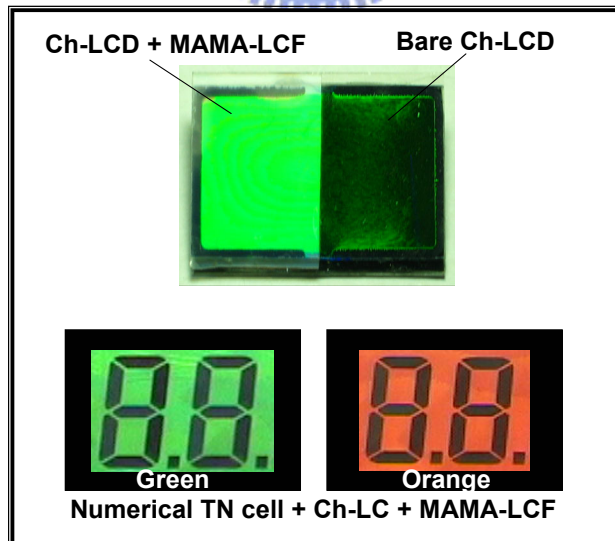
The photographs of displayed images using the MAMA-LCF on a color STN-LCD, PDLC and Ch-LCD, taken under ambient condition are shown in the Figs. 4-17(a), (b) and (c), respectively. In comparison, Fig. 4-17(a) is the photograph of STN-LCD with an MAMA-LCF (left) and an 80% haze diffuser (right), which is commonly used to enhance the brightness of mobile displays. The photographs of PDLC with MAMA light control film and a bare PDLC are shown in Fig. 4-17 (b). Additionally, Fig. 4-17(c) displays the two-surface buffed Ch-LCD with and without MAMA-LCF, and also the photos of using MAMA-LCF on a conventional numerical TN panel by injected Ch-LC material, which reflected green and orange colors, respectively. The high image quality by the MAMA-LCF on the three different LCDs is clearly demonstrated.



(a)



(b)



(c)

Fig. 4-17. Sample photographs of (a) color-STN LCD, (b) PDLC, and (c) Ch-LCD. The displays with MAMA-LCF clearly show much better image quality. (Color photos are shown in appendix)

4.6 Random grating LCF for larger size portable LCDs

We have developed a modified multi-directional asymmetrical microlens array light control film (MAMA-LCF) to increase the brightness and contrast ratio of reflection-type display, by cutting along microlens array's diametric direction to form an off-axis one with multi-directional arrangement. The lens structure of MAMA-LCF can collect and redirect the reflected light into lower viewing region resulting in a very high brightness image. Nevertheless, such a lens structure also focused the reflected light to a specific viewing angle, which is very suitable for mobile phone size panel. To further extend the applications of light control film for larger size panel (> 4 inches), we need to widen the viewing angle with high uniformity. Additionally, compared with white paper, the displayed images of conventional reflective LCDs still have inadequate whiteness. From the analyses, only the reflectance between $0.6x$ and $1.5x$ of MgO standard white can result in a paper white image^[80]. Consequently, the reflectance-profile-controlled components should be well designed to maintain the reflectance between $0.6x$ and $1.5x$ of MgO, keeping the image “paper white”.

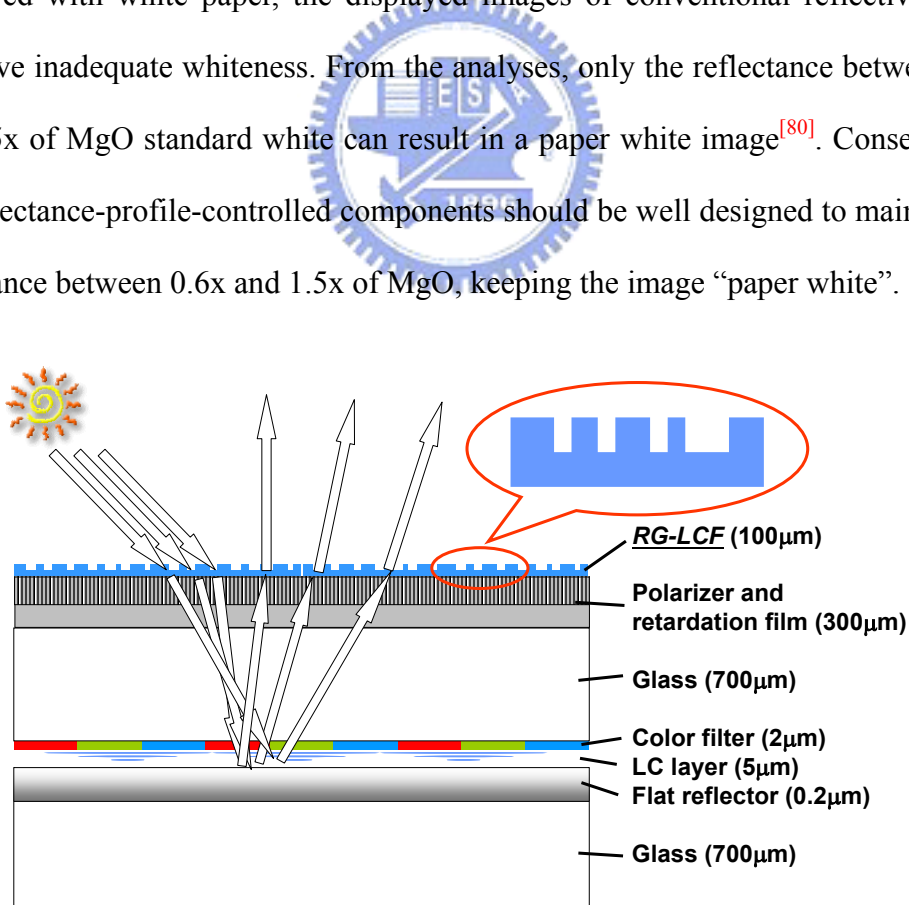


Fig. 4-18. Optical configuration of a reflective LCD with the RG-LCF laminated onto the front surface.

Therefore, we proposed another reflectance-profile-controlled component “random grating light control film (RG-LCF)”, which also can be easily laminated onto the top surface of a reflective LCD to control the light distribution, as schematically shown in Fig. 4-18, for yielding wide viewing angle, high uniformity, and paper white image.

4.6.1 Optical design of RG-LCF

The structures on the proposed film are randomly arranged gratings, which simulate the irregularly distributed fiber structures of a paper, yet can control the reflective light distribution using properly designed grating pitches and orientations. The gratings were designed to have pitches from 2 to 8 μm and nine different orientations ranging from -40° to $+40^\circ$ with a 10° period, as shown in Fig. 4-19. Additionally, the size of each grating is $25 \times 25 \mu\text{m}^2$ and the arrangement in a single pixel is randomized to avoid the moiré patterns and color dispersion.

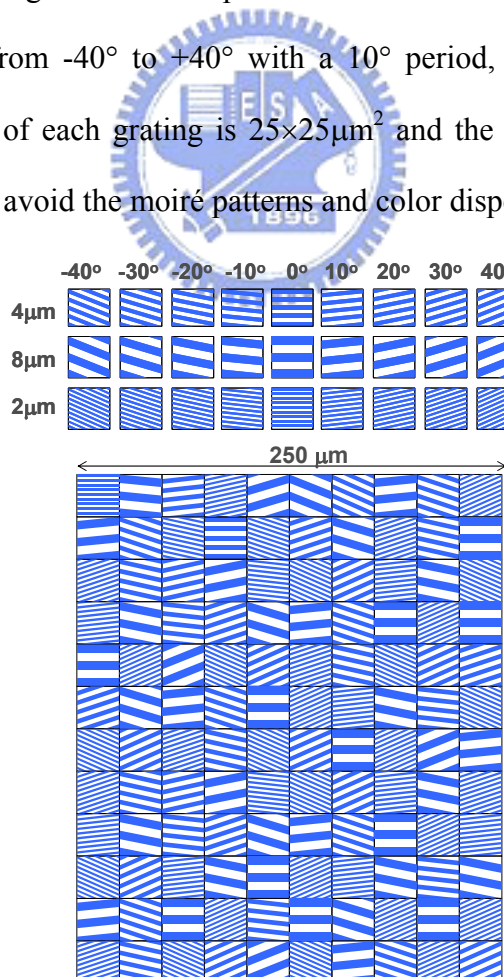
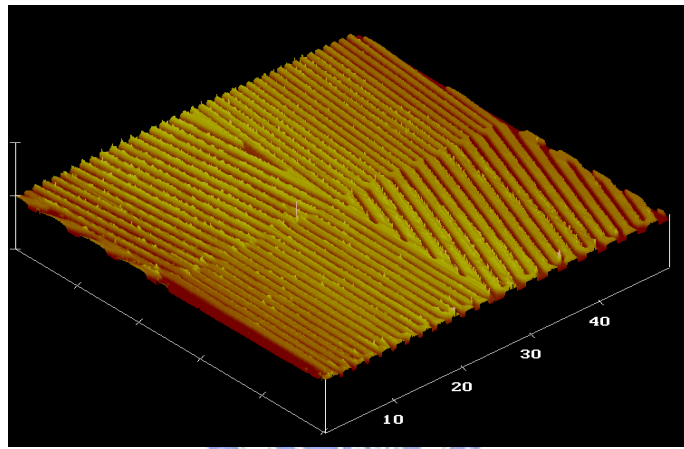


Fig. 4-19. The designed pattern of random grating LCF for a reflective LCD.

4.6.2 Experimental results of RG-LCF

As MAMA-LCFs, RG-LCFs are easily fabricated by standard semiconductor processes and injection/stamping molding. By using these well-developed fabrication processes, the designed grating structure can be produced economically and reproducibly in large volume. The fabricated structure of random grating light control film (RG-LCF) was as the AFM image shown in [Fig. 4-20](#).



[Fig. 4-20.](#) The 3D view of random grating LCF measured by using AFM.

The reflected light profiles of a reflective color STN-LCD with RG-LCF and MAMA-LCF are represented as the solid and dash line in [Fig. 4-21](#), respectively. For a collimated illumination from -30° , the specular reflection occurs at 30° . The idealized reflective profile for a 4-inch reflective panel, as the dot line illustrated in [Fig. 4-21](#), shall has the reflectance of $0.8x$ MgO, which is the reflectance of white paper, from 0° to 20° . Obviously, the one using RG-LCF provides more uniform reflectance profile than that of MAMA-LCF within typical viewing region from 0° to 20° , with high reflectance. It also illustrates that using the laminating RG-LCF, the reflectance of the R-LCD in viewing angles from 5° to 20° can be effectively controlled to be $0.6x$ to $1.5x$ of MgO, achieving a whiteness appearance close to

standard white. Additionally, the reflective image is successfully being separated from the specular reflection by using RG-LCF. Consequently, with laminating the RG-LCF, the LCD can yield high performance reflective images.

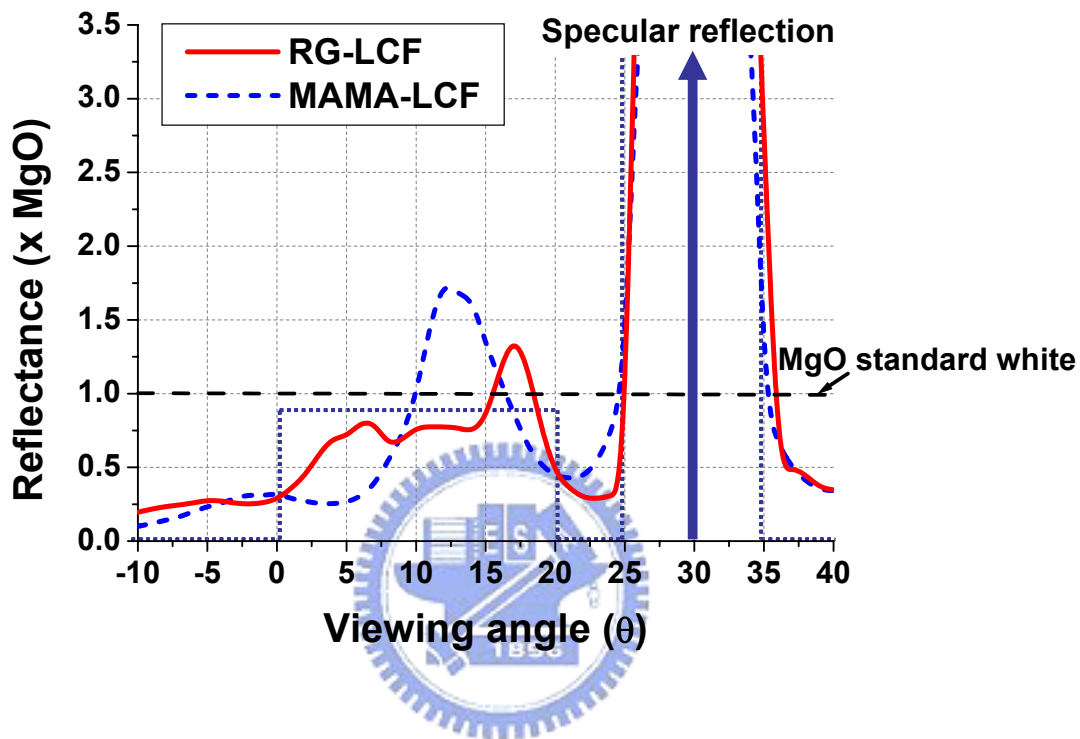


Fig. 4-21. Reflectance profile of the random grating light control film laminated on a reflective LCD.

4.7 Discussion

Many image enhanced components for reflective displays have been proposed and used. These components are generally divided into two categories; diffusive (RG-LCF^[74], bump reflector^[70] and diffuser^[69]) and collective (MAMA-LCF^{[72],[73]}, micro slant reflector^[81], and holographic film^[82]). The comparison of their respective performance among LCFs and other components is listed in Table. 4- 3. Bump reflector can provide the high image quality with high brightness, very good contrast ratio and wide viewing angle, yet it requires very complex fabrication process which

results in a high cost. Diffuser has the lowest price; nevertheless, it's image quality is not so good as other approaches. Slant reflector, and holographic film can display very high brightness yet the viewing angle is only acceptable. RG-LCF and MAMA-LCF display almost the same image quality with bump and slant reflector, respectively. Light control films, however, utilizes a well-developed semiconductor process and stamp molding to reduce the fabrication cycle. Plastic film is used as the substrate, thus the material cost is low. Furthermore, the film-like component can be laminated on most kinds of the reflective displays that extend the competitiveness of LCFs.

Table. 4-3. Comparison of conventional image enhanced components used for reflective displays.

Compared items	Diffusive type			Collective type		
	RG-LCF	Bump	Diffuser	MAMA-LCF	Slant reflector	Holographic film
Brightness	High	High	Low	Very high	Very high	Very high
Contrast ratio	Good	Very good	Poor	Good	Very good	Good
Viewing angle	Wide	Wide	Narrow	Acceptable	Acceptable	Acceptable
Fabrication process	Easy	Very complex	Very easy	Easy	Complex	Complex
Fabrication time	Very short	Very long	Short	Very short	Long	Short
Cost	Low	Very high	Very low	Low	High	High
Applicable displays	TFT STN PDLC Ch-LCD	TFT STN PDLC Ch-LCD	STN PDLC Ch-LCD	TFT STN PDLC Ch-LCD	TFT STN PDLC	TFT STN PDLC Ch-LCD

4.8 Summary

Conventional reflective LCDs are of low brightness, poor contrast ratio, narrow viewing angle, and inadequate uniformity. On the one hand, the use of MAMA-LCF effectively enhances the display brightness and contrast of reflective color-STN (1.5X

MgO, CR~15), PDLC (2.8 X MgO, CR~23) and Ch-LCD (2.8 X MgO, CR~13) under ambient light condition. On the other hand, the RG-LCF provides more uniform reflectance profile from 0° to 20° viewing angle with high reflectance (0.8x MgO). Therefore, the two LCFs have their own applications for improving the reflective image qualities. Additionally, by using optimized design, the color dispersion, and moiré patterns, that may be caused by the micro-components, are all invisible. The surface scattering can also be reduced by coating an index matching material - EGC1700 (n=1.38).

The LCFs can be easily fabricated by semiconductor processes and injection/stamping molding. By using these well-developed fabrication processes, the designed microlens or grating structure can be produced economically on thin transparent plastic substrate.

